HEAT TRANSFER IN A REAL ENGINE ENVIRONMENT

Herbert J. Gladden
NASA Lewis Research Center
Cleveland, Ohio

INTRODUCTION

Improved performance of turbojet and turbofan engines is typically accompanied by increased cycle pressure ratio and combustor exit temperature. The continuing increase in turbine entry gas pressure and temperature as well as the high development cost puts a premium on an accurate initial aerothermal design of the turbine hot section hardware. The design goals for commercial jet engines include high cycle efficiency, increased durability of the hot section components (lower maintenance costs), and lower operating costs (increased thrust-to-weight and lower SFC). These goals are contradictory in that high cycle efficiency requires minimizing bleed air for cooling while the heat load is being increased. And durability requires the component metal temperatures and temperature gradients to be minimized. An optimum design can only be realized through an improved understanding of the flow field and the heat-transfer process in the turbine gas path.

The sophisticated computer design codes being developed have the potential of providing the designer with significantly better estimates of the flow field and the heat load on the hot-section components. These codes are evaluated and verified through low-temperature and pressure research in cascades and tunnels. However, by design, these facilities do not model all of the processes that exist in a real engine environment, and therefore, the ability of the design codes to predict the interaction of the various parameters cannot be fully evaluated.

A significant portion of the HOST project has been to develop instrumentation that can be used in a real engine environment to measure the boundary conditions of the flow field and heat-transfer process. The hot section facility (HSF) at NASA Lewis provides a "real engine" environment and convenient access for advanced instrumentation to evaluate these instruments. In addition, it provides an opportunity to study the aerothermal performance of turbine hot section components.

Several advanced instrumentation concepts developed into functional hardware under both the HOST program and independent programs were recently evaluated in the HSF. These instruments included thin-film thermocouples, two types of heat flux sensors, and a dynamic gas temperature probe. In addition, airfoil surface temperatures were measured by an infrared-film technique and by an optical pyrometer.

The thermal performance of a full-coverage film-cooled stator airfoil was also evaluated in this research program. The tests were conducted at chord-length Reynolds numbers of 0.5 to 2.5 million which correspond to typical advanced engine conditions. This corresponds to gas temperature and pressure levels up to 1500 K and 17.7 atm.

FACILITY

The HSF has fully automated control of the research rig through an integrated system of minicomputers and programmable controllers. The major components of this facility and how they interface to provide a real engine environment are discussed in more detail in references 1 and 2.

Combustion air is provided to the facility at 10 atm through a nonvitiated preheater which modulates the air temperature between ambient and 560 K. A 20-atm mode of operation provides combustion air at pressures up to 20 atm and temperatures up to 730 K when using the heat of compression of a 2:1 compressor.

A cross-sectional schematic of the HSF cascade is shown in figure 1. The major components shown consist of a heat source (combustor), the full-annular vane row, an exhaust duct, a quench system (to lower exhaust-gas temperature), and the exhaust system. The vane row consists of 36 stator vanes separated into two groups: 10 test vanes and 26 slave vanes. The test vane and slave vane cooling airs are supplied from two separate manifolds with the flow rates to each manifold independently computer controlled.

The thermal performance of a full-coverage film-cooled vane is discussed in reference 1. The airfoil for these tests is shown in figure 2. The advanced instrumentation evaluation tests were conducted using a hollow airfoil shell with a solid surface. A typical airfoil for these tests is shown in figure 3.

INSTRUMENTATION

The advanced instrumentation evaluated consisted of thin-film thermocouples, Gardon-type and embedded thermocouple heat flux gauges, a dual-element dynamic gas-temperature probe, and two types of infrared surface-temperature measuring devices. Thin-film thermocouples installed on a hollow shell airfoil pressure surface are shown in figure 3. The thermal elements were platinum/platinum - 10 percent rhodium (type S) sputtered on a substrate of Al_2O_3.

Two types of heat flux gauges were installed on the airfoil pressure surface: gardon-type gauges and paired thermocouple type gauges. These gauges were installed and calibrated by Pratt & Whitney Aircraft following the procedure outlined in reference 4. A step-wise procedure for installing the gardon-type gauges is depicted in figure 4.

The dual-element dynamic gas temperature probe was located at the combustor exit. The two thermal elements of the probe were platinum - 30-percent rhodium/platinum - 6-percent rhodium (type B) and were 0.076 and 0.25 mm in diameter. The probe elements are shown in figure 5, and its construction details are discussed in reference 5.

Airfoil surface temperatures can be determined by infrared radiation emitted from the hot surfaces. The two techniques described in reference 6 are based on an infrared-photography system or a photoelectric scanning system. The infrared-photography system was designed primarily for temperature measurements in stationary systems and was used for turbine-vane leading-edge region measurements. The photoelectric scanning system was developed primarily for temperature measurement in rotating systems, but during the cascade tests it was adapted to measure

temperatures on the vane trailing-edge surface. These two systems are shown schematically in figures 6 and 7.

RESULTS AND DISCUSSION

Thermal Scaling

During the development of an engine, the turbine components are frequently tested at lower temperature and pressure in cascades and tunnels to verify the heat-transfer design. There has been concern for the validity of these data and whether the thermal scaling laws are sufficiently satisfied between the rig tests and the actual engine. Data were taken over a wide range of temperatures and pressures to investigate the thermal scaling phenomena. The primary parameters held constant were Reynolds number and Mach number. The results are shown in figure 8. A midspan average cooling effectiveness parameter φ for the full-coverage film-cooled vane is shown as a function of the coolant-to-gas flow ratio.

The lowest Reynolds number data taken (0.5×10^6) are presented in figure 8(a). A trend is shown by these data where the higher gas-temperature data have a lower cooling effectiveness than the lower gas-temperature data. The difference in cooling effectiveness values is about 0.02 at a coolant-to-gas flow ratio of 0.113.

The data shown in figure 8(b) represent a higher Reynolds number (1.25×10^6) and are characteristic of both engine operation (high-gas temperature) and rig tests (low-gas temperature). These data show a trend similar to the data in figure 8(a); that is, the low gas temperature data (rig tests) have a slightly higher cooling effectiveness than the higher gas temperature data (engine conditions). The difference in cooling effectiveness values is about 0.02 at a coolant-to-gas flow ratio of 0.11.

Reference 7 predicts up to a 0.04 increase in cooling effectiveness from engine conditions to lower temperature rig-test conditions. This phenomenon was shown to result from our inability to thermally scale the material thermal conductivity. This trend is shown by both Reynolds number data sets. It can be concluded from these data and reference 7 that low-temperature rig tests are somewhat optimistic in predicting the cooling performance of a design prototype operating at engine conditions.

Infrared Temperature Measurement

A thermal image of an airfoil leading edge and pressure surface are shown in figure 9. The gray tones represent the temperature of the airfoil through its thermal energy output. The lightest regions are at high temperatures and the dark regions are cooler. The procedures for recording and interpreting thermal image is discussed in reference 6. The gray tones in the figure indicate a hot leading edge and a relatively uniform and lower temperature on the pressure surface. The pattern of dark spots on the leading edge of vane 3 are the film cooling holes. In addition, a horseshoe-vortex type thermal pattern can be seen on the hub endwall as it wraps around the leading edge of the vane.

Heat-Transfer Coefficients

Heat-transfer coefficients were determined by repeatedly ramping the gas temperature between a low and a high temperature at several frequencies and recording the transient response of the wall temperature. A portion of typical wall and gas temperature time histories (fig. 9) illustrates the magnitude and shape of the transient input and the time response of the thin film thermocouple. Typically, the gas temperature was varied 140 K, and the wall temperature responded with a variation of 30 K. In figure 10 six repetitions of a 2-sec ramp cycle are followed by seven repetitions of a 4-sec ramp cycle. These and other ramp-cycle lengths were used to gather data at fundamental frequencies from 0.005 to 0.5 Hz (periods of 200 to 2 sec).

The amplitude ratio of the Fourier components of the wall to gas temperatures was determined from a cross-correlation of the temperature histories. The data follow a slope of -1/2 and has a phase lag of about 45° as Dils' theory requires, justifying the use of that approximation to determine local heat-transfer coefficients. The coherence function between the gas-temperature ramp and the wall-temperature response was greater than 0.8, which indicates that there was a significant relationship. The trend of increased heat transfer with increased Reynolds number is also indicated by the data.

The experimental heat-transfer coefficients on the airfoil pressure and suction surfaces are shown in figures 10 and 12. The data are plotted as a function of the dimensionless surface distance, x/L. Also included on the figure is an analytical solution from the STAN5 boundary layer code.

Pressure surface. - The low Reynolds number data (0.55×10^6) of figure 11 show generally laminar characteristics in the midchord region with a transition to turbulent flow near the trailing edge. The steady-state experimental data from the Gardon-gauges and the paired thermocouples also show generally laminar characteristics in the midchord region with a magnitude of ~75 percent of the transient data. The experimental data are also compared with an analytical solution that has been forced to a turbulent flow solution near the airfoil leading edge. This solution compares favorably with the steady-state heat-transfer coefficients, but it is ~75 percent of the transient data.

The 1.2×10^6 Reynolds number data (fig. 11) follow a trend suggesting boundary-layer transition in the midchord and trailing-edge regions. However, the heat-transfer coefficients in the leading-edge region have relatively large magnitudes, which is consistent with an augmented laminar boundary layer. The two transient measurements at x/L of 0.354 are from different vanes and show a significant difference in magnitude. Data up to an x/L of 0.354 are in an apparent transitional region indicated by the steep gradient in the heat-transfer coefficient. The steady-state experimental data from the Gardon-type and paired-thermocouple gauges generally compare with the transient experimental data. The STAN5 analysis was also forced to a turbulent flow solution near the leading edge for this Reynolds number. The results (fig. 11) show a good comparison between the analysis and the experimental data in both magnitude and trend.

Data for a Reynolds number of 1.9×10^6 show the heat-transfer coefficients from both the transient and the steady-state measurements to have the same trend in the midchord region (fig. 11). However, the steady-state data have a larger magnitude than the transient data at this Reynolds number, which is opposite of the relation shown in the lower Reynolds number data. The analytical solution shows a good

comparison with the experimental heat-transfer coefficients when the boundary layer is forced to a turbulent flow solution near the leading edge.

Suction surface. - Experimental heat-transfer coefficients from the transient technique are shown in figure 12 for the airfoil suction surface. The analytical solution from STAN5 follows the data reasonably well for all three Reynolds numbers. However, at an x/L of 0.82, the experimental heat-transfer coefficient shows a substantial increase over the trend established by the other data. A sudden increase in heat transfer on a suction-surface trailing edge is not uncommon and may be due to secondary flow effects. In addition, the analytical solution generally underpredicts the experimental results, and the magnitude of the underprediction increases with decreasing Reynolds number.

The transient and steady-state experimental data on both the airfoil pressure surface and the transient data on the suction surface show increasing magnitude with Reynolds number as would be expected. In addition, the experimental data trends are similar to those predicted by the STAN5 boundary-layer code. Data from both transient and steady-state techniques on the pressure surface have similar magnitudes and trends. There is, however, a significant deviation in magnitude between the experimental heat-transfer coefficients and those predicted by STAN5 in the laminar and transitional regions.

CONCLUSIONS

The experimental data-base for the evaluation of sophisticated computer design codes for the turbine hot section components must include data at real engine conditions. Part of the HOST program has been directed toward the development of instrumentation capable of measuring boundary conditions of the flow field and heat-transfer process in the hostile environment of the turbine. The hot section facility at the Lewis Research Center was used to demonstrate the capability of these instruments to make the required measurements. The results of thermal scaling tests show that low-temperature-and-pressure rig tests give optimistic estimates of the thermal performance of a cooling design, for high-temperature-and-pressure application. The results of measuring heat-transfer coefficients on turbine vane airfoils through dynamic data analysis show good comparison with measurements from steady-state heat-flux gauges. In addition, the data trends are predicted by the STAN5 boundary-layer code. However, the magnitude of the experimental data was not predicted by the analysis, particularly in laminar and transitional regions near the leading edge. The infrared-photography system was shown capable of providing detailed surface thermal gradients and secondary flow features on a turbine vane and endwall.

REFERENCES

1. Gladden, H.J.; Yeh, F.C.; and Fronek, D.L.: Heat Transfer Results and Operational Characteristics of the NASA Lewis Research Center Hot Section Cascade Test Facility. ASME Paper 85-GT-82, Mar. 1985.

2. Cochran, R.P.; Norris, J.W.; and Jones, R.E.: A High-Pressure, High-Temperature Combustor and Turbine Cooling Test Facility. ASME Paper 76-WA/GT-4, Dec. 1976.

3. Gladden, H.J.; and Proctor, M.P.: Transient Technique for Measuring Heat Transfer Coefficients on Stator Airfoils in a Jet Engine Environment. AIAA Paper 85-1471, July 1985.

4. Atkinson, W.H.; Cyr, M.A.; and Strange, R.R.: Turbine Blade and Vane Heat Flux Sensor Development, Phase I. (PWA-5914-21, Pratt & Whitney Aircraft; NASA CR-168297) August 1984

5. Elmore, D.L.; Robinson, W.W.; and Watkins, W.B.: Dynamic Gas Temperature Measurement System Final Report Volume 1 Technical Effort. (PWA/GPD-FR-17145-Vol. 1, Pratt & Whitney Aircraft, NASA CR-168267-Vol. 1) May 1983

6. Pollack, F.G.; and Cochran, R.P.: Temperature and Pressure Measurement Techniques for an Advanced Turbine Test Facility. Measurement Methods in Rotating Components of Turbomachinery, B. Lakshminarayara and P. Runstadler, Jr., eds., ASME, 1980, pp. 319-326.

7. Gladden, H.J.: Extension of Similarity Test Procedures to Cooled Engine Components with Insulating Ceramic Coatings. NASA TP-1615, 1980.

HSF CASCADE CROSS-SECTION SCHEMATIC

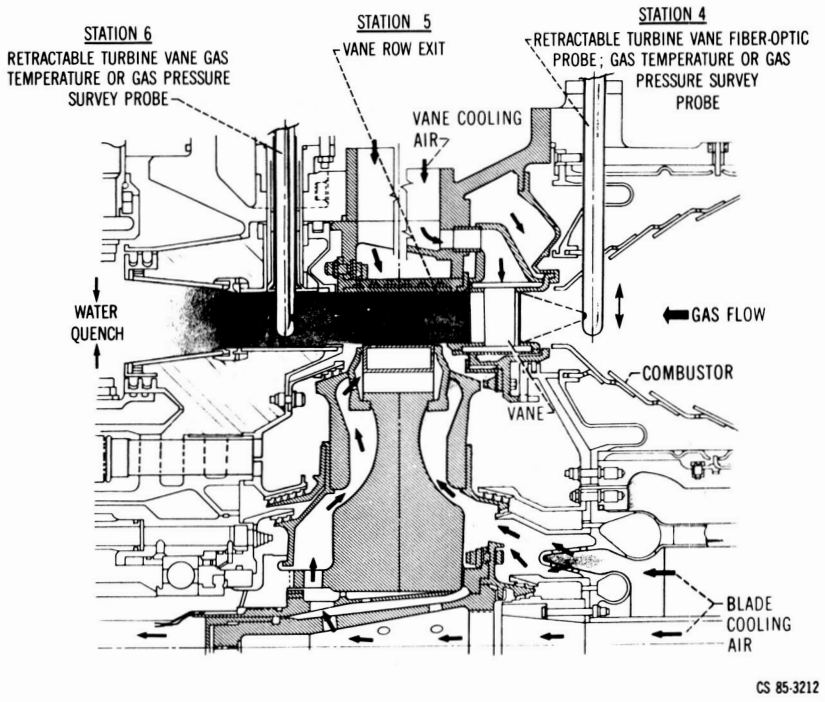

Figure 1

FULL-COVERAGE FILM COOLED VANES

USED FOR THERMAL SCALING TESTS

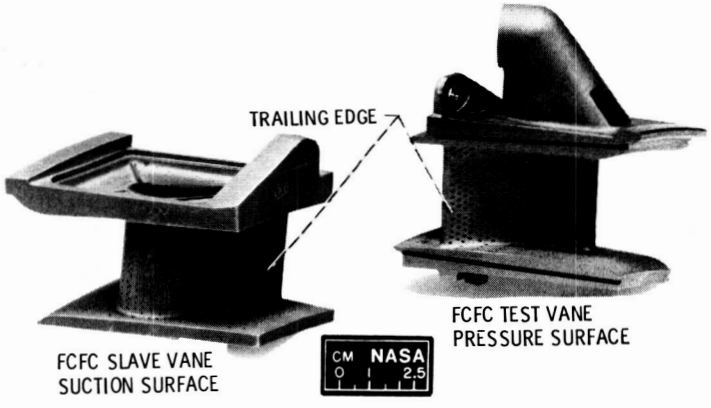

Figure 2

THIN FILM THERMOCOUPLE INSTALLATION

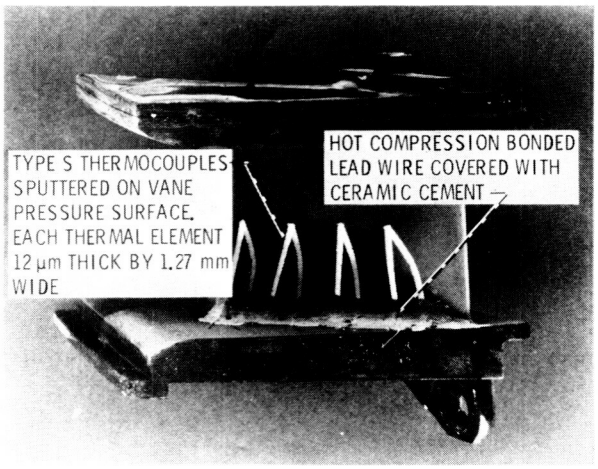

CS 85-3207

Figure 3

HEAT FLUX GAGE INSTALLATION IN VANE

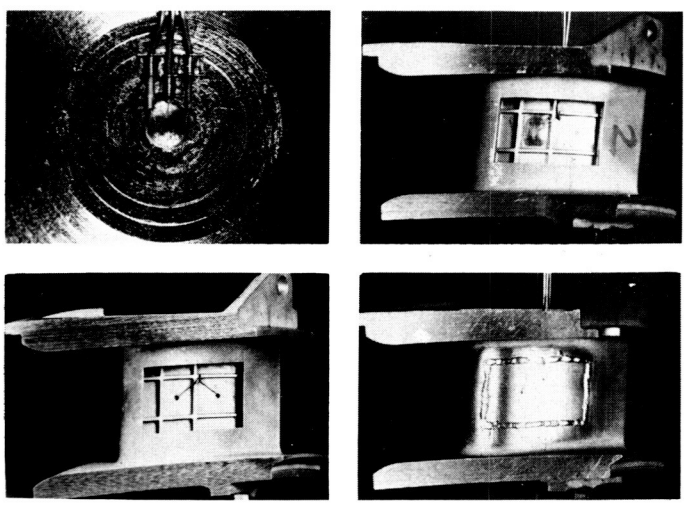

Figure 4

DUAL-ELEMENT GAS TEMPERATURE PROBE

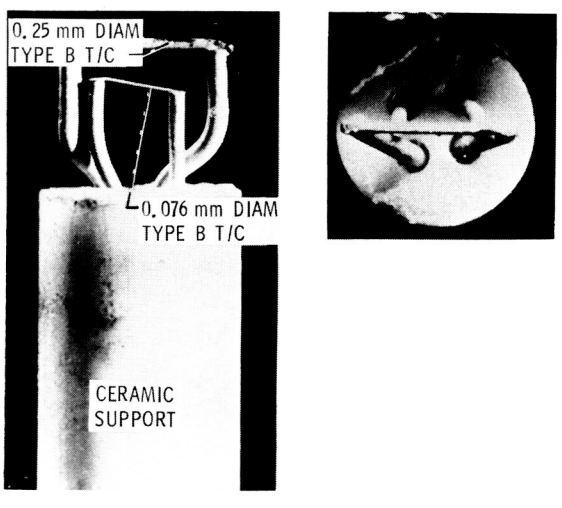

Figure 5

PHOTOELECTRIC SCANNING SYSTEM FOR ROTATING BLADES

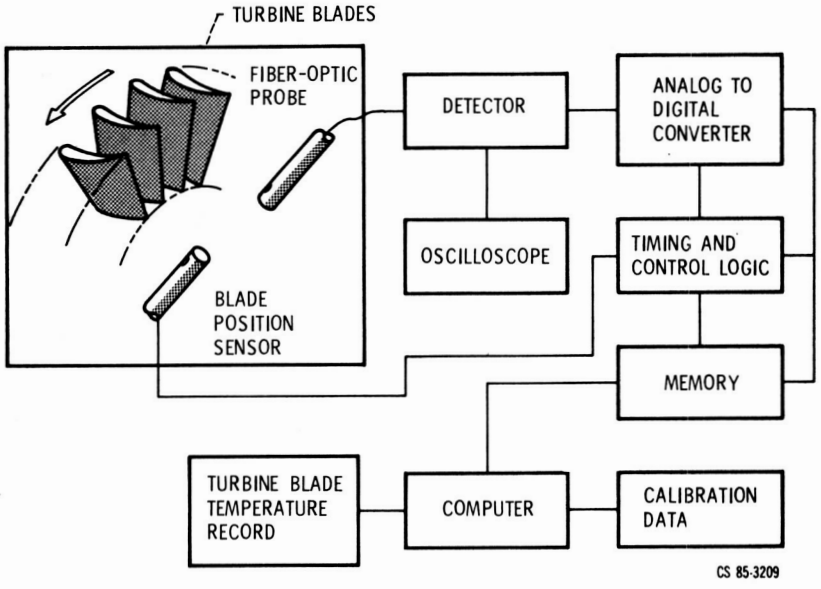

Figure 6

PHOTOGRAPHY SYSTEM FOR STATIONARY VANES

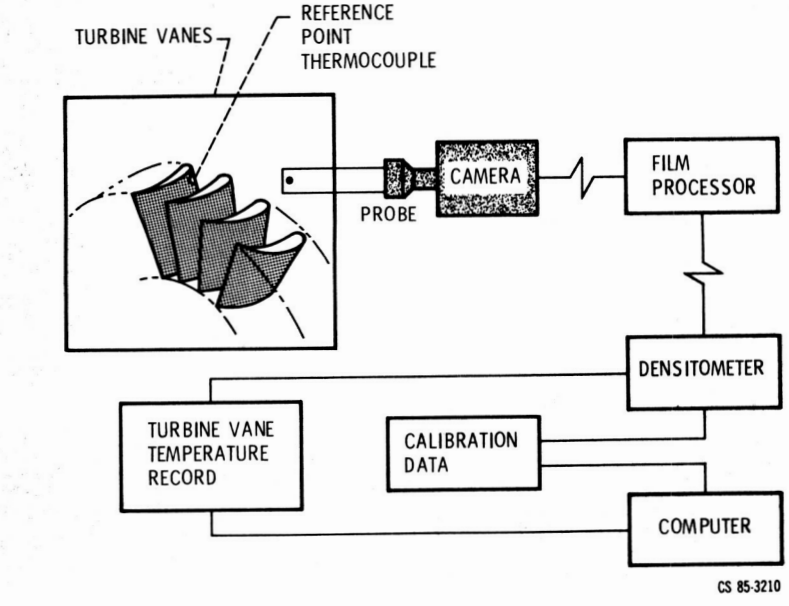

Figure 7

THERMAL SCALING RESULTS FROM FULL-COVERAGE FILM-COOLED VANE AIRFOIL

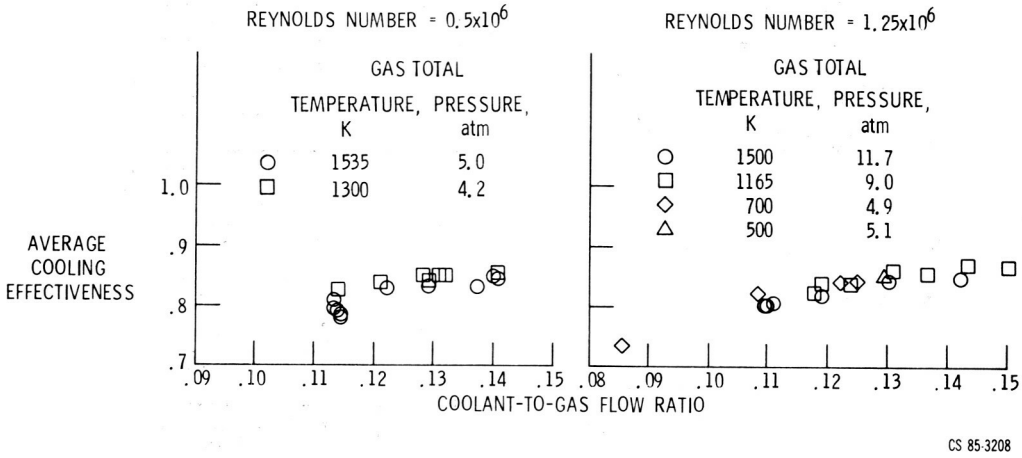

Figure 8

FULL-COVERAGE FILM-COOLED VANE AIRFOIL THERMAL IMAGE

IR PHOTOGRAPHY SYSTEM

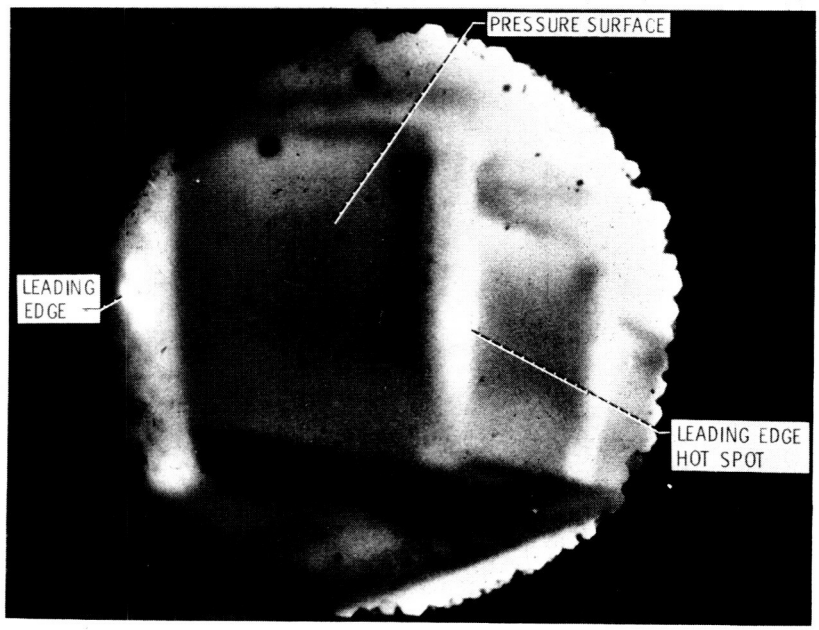

Figure 9

TYPICAL TIME HISTORIES OF GAS AND WALL TEMPERATURES

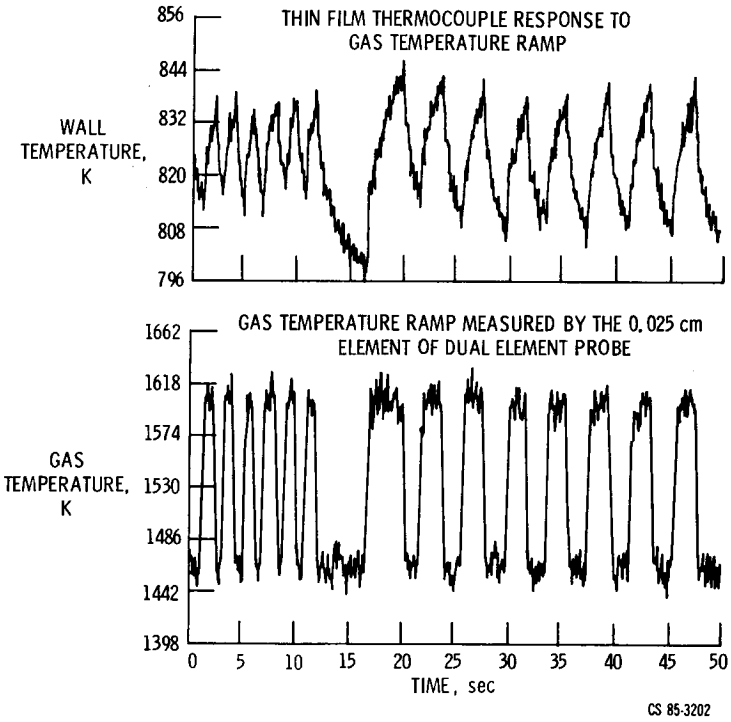

Figure 10

EXPERIMENTAL HEAT TRANSFER COEFFICIENTS ON VANE AIRFOIL PRESSURE SURFACE

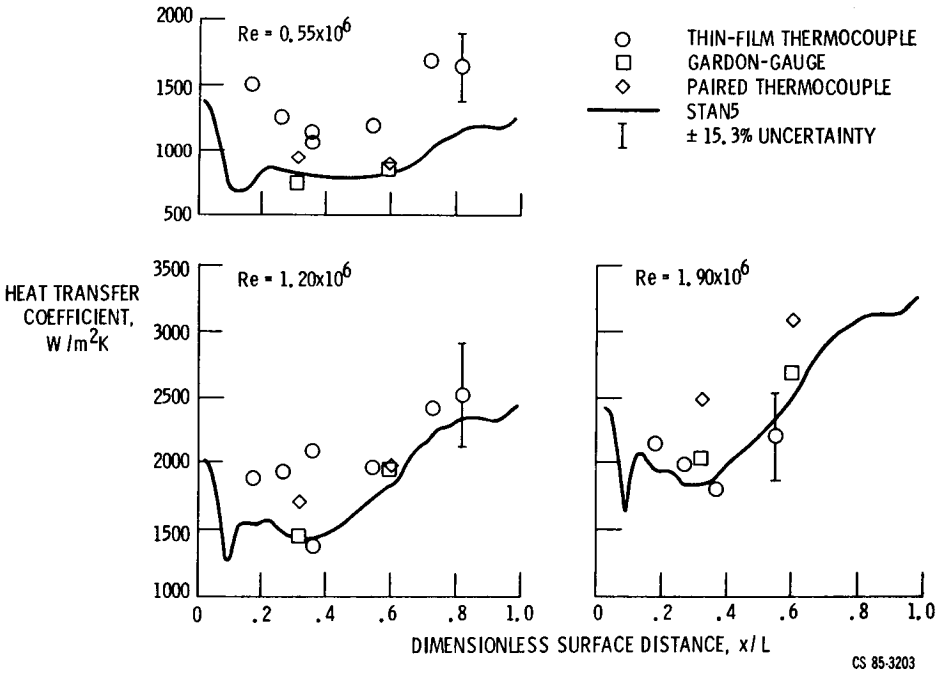

Figure 11

EXPERIMENTAL HEAT TRANSFER COEFFICIENTS ON AIRFOIL SUCTION SURFACE

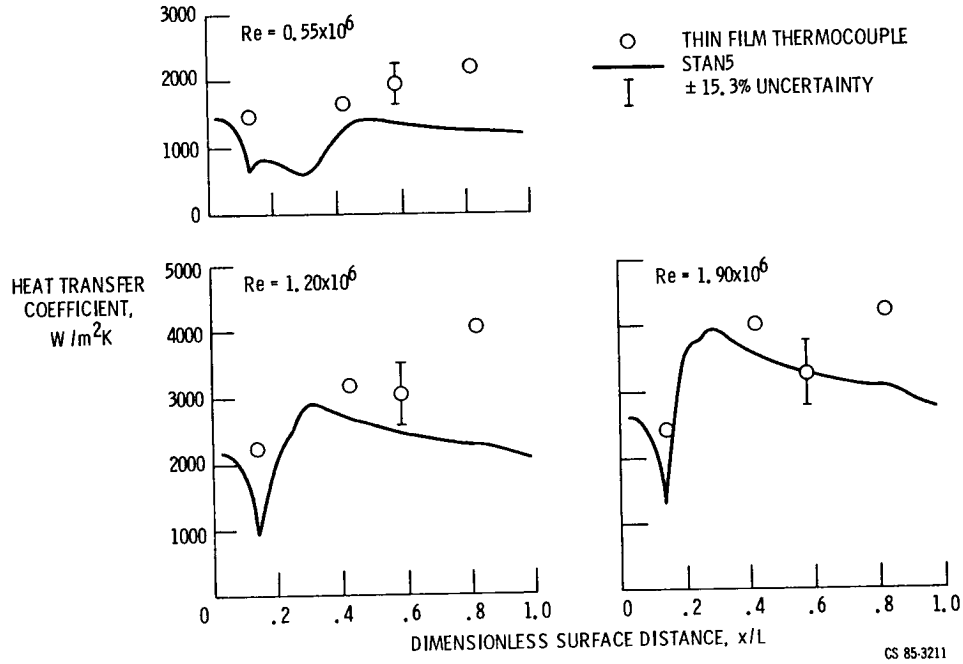

Figure 12